IOSR Journal Of Applied Physics (IOSR-JAP)
e-ISSN: 2278-4861.Volume 13, Issue 4 Ser. I (Jul. – Aug. 2021), PP 08-14
www.Iosrjournals.Org

Band Alignment of Type II Strained $GaAs_xSb_{1-x}/Ga_yIn_{1-y}As$ Quantum Well on $InP(001)$ substrate

Ugochukwu Joseph, C.I Oriaku*, A.D Asiegbu., E.C Nwaokorongwu, Uchechi K.P.Okpechi
Department of Physics, College of Physical and Applied Sciences, Michael Okpara University of Agriculture, Umudike

Abstract:
In nature every semiconductor material needs to be doped. Sometimes to nearly degenerate level, eg. In applications such as thermoelectric, transparent, electronics or power electronics. However, many materials with finite band gaps are not dopable at all, while many others exhibit strong preferences towards allowing either p-type or n-type doping, but not both. In this work we develop a model of strained InGaAs/GaAsSb double barrier quantum well heterostructure on InP substrate using the model solid theory. The matlab program model was used to obtain the conduction and valence band offsets and their ratios,. These were obtained theoretically by employing experimental binary band parameters obtained from literatures
Key Word*: Band Offsets; Intrinsic; Electron concentration; Strained Conduction Band.*

Date of Submission: 10-07-2021 Date of Acceptance: 26-07-2021

I. Introduction

The use of semiconductor alloys and heterojunctions in recent years have led to the development of major optoelectronic devices and detectors. Both theoretical and experimental researches have been carried out on the properties of these materials/alloys in their applications. For instance low bandgap materials are required for infrared detectors. The growth of these vital alloys (method of deposition) has a role to play in its composition and modification of these material properties. These methods of growth have helped produced alloys not only when the lattices are matched but also when they have different lattice constant [1]. Quantum wells are heterostructures in which a narrow bad gap thin layer with low potential energy of one semiconductor is sandwiched between two layers of a different semiconductor material, thereby forming a *heterojunction* [2] . An essential feature is that the two semiconductors must have different energy gaps for optical applications, and different refractive indices. The well materials are chosen such that electrons available for conduction in the middle layer should have lower energy compared to that of the outer layers. This creates an energy dip (or well) that confines the electrons in the middle layer [3] .

GaAs, GaSb, InP, InAs semiconductors exhibit cubic symmetry [4] with zinc blende or sphalerite structure, with fcc lattice interpenetrating each other [5]. They are all having direct band gaps. GaInAs/GaAsSb quantum well is a type II heterojunction with an effective conduction band gap as small as 0.3 eV when lattice matched InP. It is suitable for infrared generator and infrared detectors [6] . Its band offset is an essential parameter in interfacial structure which decides both transport and quantum confinement [7].

II. Material And Methods

In growing a material on a substrate, the substrate and the layer ought to have the same crystalline structure. They should not differ too much in lattice constants. If they do the heterojunction formed will be strained which may result to dislocation [8]. In the absence of strain, if two material forms a heterojunction with approximately same lattice constant or are lattice matched, the band lineup will determine how the band structure of the two materials line up at the interface which later produces values for the band discontinuities [9] . The position of the topmost valence band of each will be given by [10]

$$E_v = E_{v,av} + \frac{\Delta_0}{3} \quad (1)$$

While the split- off band-edge energy is given as

$$E_{Sp.O} = E_{v,av} - \frac{2\Delta_0}{3} \quad (2)$$

where Δ_0, is the spin-orbit splitting energy, $E_{v,av}$ is the average valence band energy and E_v, the valence band energy. The conduction band is obtained by summing the valence band and the band gap of the material. ie

$$E_c = E_v + E_g \quad (3)$$

The band lineup between these two materials 1 and 2 will be given by

$$\Delta E_g = E_g^1 - E_g^2 \quad (4)$$

while the band-edge discontinuities is given by [11]

$$\Delta E_c = E_c^1 - E_c^2 \qquad \Delta E_v = E_v^2 - E_v^1$$
$$\Delta E_c + \Delta E_v = \Delta E_g \quad (5)$$

The ratios of the band-edge discontinuities, $Q_c = {\Delta E_c}/{\Delta E_g}$ and $Q_v = {\Delta E_v}/{\Delta E_g}$ are obtained from the theory and can be compared with experimental data

If a material with a lattice constant a_m is grown on a substrate with a lattice constant a_s such that the lattice constant are not the same along the z direction, we have the tensile strains $\varepsilon_{xx} = \varepsilon_{yy} = \frac{a_s - a_m}{a_m}$ and $\varepsilon_{zz} = -2\frac{C_{12}}{C_{11}}\varepsilon_{xx}$ for 001where C_{12} and C_{11} are the elastic stiffness of the material.

The hydrostatic strain corresponds to the change in volume

$$\varepsilon_{hydro} = \frac{\Delta V}{V} = \varepsilon_{xx} + \varepsilon_{yy} + \varepsilon_{zz} \quad (6)$$

The band edge shift are

$$\Delta E_{v,av} = a_v \varepsilon_{hydro} = -P_\varepsilon = 2\varepsilon_{xx} a_v (1 - \frac{C_{12}}{C_{11}}) \quad (7)$$

$$\Delta E_c = a_c(\varepsilon_{xx} + \varepsilon_{yy} + \varepsilon_{zz}) = P_c = 2\varepsilon_{xx} a_c (1 - \frac{C_{12}}{C_{11}}) \quad (8)$$

The position of the average energy of the valence band $E_{v,av}$ under strain is shifted from its unstrained position $E_{v,av}^0$ by $= -P_\varepsilon$ is

$$E_{v,av} = E_{v,av}^0 - P_\varepsilon \quad (9)$$

We thus have the center of the valence-band-edge energy

$$E_v = E_{v,av} + \frac{\Delta}{3} = E_v^0 - P_\varepsilon \quad (10)$$

the heavy-hole, light hole and spin-orbit split-off band edges are

$$E_{HH} = E_v^0 - P_\varepsilon - Q_\varepsilon \quad (11)$$

$$E_{LH} = E_v^0 - P_\varepsilon - \frac{\Delta}{2} + \frac{Q_\varepsilon}{2} + \frac{1}{2}[\Delta^2 + 2\Delta Q_\varepsilon + 9Q_\varepsilon^2]^{1/2} \quad (12)$$

$$E_{SO} = E_v^0 - P_\varepsilon - \frac{\Delta}{2} + \frac{Q_\varepsilon}{2} - \frac{1}{2}[\Delta^2 + 2\Delta Q_\varepsilon + 9Q_\varepsilon^2]^{1/2} \quad (13)$$

The conduction band edge is shifted by P_c given by

$$E_c = E_v^0 + E_g(z) + P_\varepsilon \quad (14)$$

Note that in the limit of a large spin-orbit split-off energy $\Delta \gg |Q_\varepsilon|$, we can ignore the coupling of the spin-orbit split-off band and [12]

$$E_{LH} = E_v^0 - P_\varepsilon + Q_\varepsilon \quad (15)$$

$$E_{SO} = E_v^0 - P_\varepsilon - \Delta \quad (16)$$

Table 1: Calculated Parameters used as computed by interpolation

Compound	GaAs	GaSb	InAs	InSb	InP
Lattice Constant at 300K (Anstrong A)	5.65325[6]	6.0959[6]	6.0583[6]	6.4794[6]	5.8697[6]
Energy band gap E_g^Γ at 300K (eV)	1.424[10]	0.812[10]	0.417[15]	0.235[10]	1.4236[10]
$E_{v,av}$ Absolute energy level	-6.92[10]	-6.25[10]	-6.67[10]	-6.09[10]	-7.04[10]
Spin-orbit splitting Δ_o	0.341[6]	0.76[6]	0.39[6]	0.81[6]	0.108[6]
Conduction band hydrostatic deformation potential a_c (eV)	-7.17[6]	-7.50[6]	-5.08[6]	-6.94[6]	-6.00[6]
Valence band hydrostatic deformation potential a_v (eV)	-1.16[6]	-0.80[6]	-1.00[6]	-0.36[6]	-0.60[6]
Elastic stiffness C_{11} (GPa)	1221[6]	884.2[6]	832.9[6]	684.7[6]	1011[6]
Elastic stiffness C_{12} (GPa)	566[6]	402.6[6]	452.6[6]	373.5[6]	561[6]
Elastic stiffness C_{44} (GPa)	600[6]	432.2[6]	395.9[6]	311.1[6]	456[6]
Valence band Offset VBO (eV)	-0.803[6]	-0.03[6]	-0.59[6]	0[6]	-0.94[6]

Table 2: Bowing parameters for ternary alloy materials for $E_g^\Gamma, \Delta_o, VBO, E_g^X, E_g^L$ and a_c

Bowing	E_g^Γ	Δ_o	VBO	E_g^X	E_g^L	a_c
GaIn_As	0.477[6]	0.15[6]	-0.38[6]	1.40[6]	0.33[6]	2.61[6]
GaIn_Sb	0.415[6]	0.10[6]	0.00[6]	0.33[6]	0.40[6]	0[6]
AsSb_Ga	1.43[6]	0.60[6]	-1.60[6]	1.20[6]	1.20[6]	0[6]
AsSb_In	0.67[6]	1.20[6]	0[6]	0.60[6]	0.60[6]	0[6]

Applying the model solid theory for $GaAs_xSb_{1-x}/Ga_yIn_{1-y}As$, the average valence (absolute value) for $GaAs_xSb_{1-x}$ *and* $Ga_yIn_{1-y}As$ can be evaluated as follows

$$E_{v,av} = x.*\,Ev,av(GaAs) + (1-x).*\,Ev,av(InAs) + 3x(1-x)[-a_v(GaAs) + a_v(InAs)].\frac{\Delta a}{a_0} \quad (17)$$

Where $\Delta a = a(GaAs) - a(InAs)$ and $a_0 = x.*\,a(GaAs) + (1-x).*\,a(InAs)$

$$E_{v,av} = y.*\,Ev,av(GaAs) + (1-y).*\,Ev,av(GaSb) + 3y(1-y)[-a_v(GaAs) + a_v(GaSb)].\frac{\Delta a}{a_0} \quad (18)$$

Where $\Delta a = a(GaAs) - a(GaSb)$ and $a_0 = y.*\,a(GaAs) + (1-y).*\,a(GaSb)$

The ternary alloy of $In_xGa_{1-x}As$ and $GaAs_ySb_{1-y}$ provides a wide continuous range of bandgap values with a small associated change in the lattice constant. The energy bandgap of $In_xGa_{1-x}As$ and $GaAs_ySb_{1-y}$ are modeled with both temperature and compositional dependence.

The compositional dependence of the principal bandgap of $In_xGa_{1-x}As$ and $GaAs_ySb_{1-y}$ shows a nonlinear increase of the bandgap with increasing Indium-content. It is modelled by the empirical equation

$$E_g^{\Gamma}(InGaAs) = xE_g^{\Gamma}(InAs) + (1-x)E_g^{\Gamma}(GaAs) + x(1-x)c_{(InGa)As} \quad (19)$$

Similarly

$$E_g^{\Gamma}(GaAsSb) = xE_g^{\Gamma}(GaAs) + (1-x)E_g^{\Gamma}(GaSb) + x(1-x)c_{Ga(AsSb)} \quad (20)$$

With x and c= -C, representing the mole ratio of In and the bowing parameter respectively. The value of the bowing can be obtained from the literature.

The temperature dependence of the bandgap modeled by the empirical Vershni equation is

$$E_g\Gamma(T) = E_g(T=0) - \frac{\alpha T^2}{T+\beta} \quad (eV) \quad (21)$$

Where α and β *are* the empirical fit parameters

The energy difference between the top of the valence band and the Γ point , $Ga_xIn_{1-x}As$ at T=0K [11] is given by,

$$E_{\Gamma} = 0.417 + 0.625x + 0.477x^2 \quad (22)$$

Table 3: Energy band gaps of InAs, GaAs, GaSb and their respective empirical fitting parameters obtained from Vurgaffman et al 2001

	Eg at 0 K, eV	α in eV	β, in K
InAs	0.417	2.76 X 10^{-4}	93
GaAs	1.519	5.405 X 10^{-4}	204
GaSb	0.812	4.17 X 10^{-4}	140

Table4: Bowing parameters for some ternary alloys obtained from Vurgaffman et al 2001

Ternary	Bowing parameter C
(GaIn)As	-0.477
(AsSb)Ga	-1.43

The carrier densities are function of the effective density of state in the appropriate band (conduction for n-type and valence for p-type), the Fermi energy level in the material (which is a function of temperature and dopant concentrations), and the temperature as given by the following equations:

$$n = N_c e^{-\frac{E_c - E_F}{K_B T}} \quad (23)$$

$$p = N_c e^{-\frac{E_F - E_V}{K_B T}} \quad (24)$$

where n is the electron density, p is the hole density, N_C is the density of states in the conduction band, N_V is the density of states in the valence band, E_C is the conduction band energy level, E_V is the valence band energy level, E_F is the Fermi energy level, $k_B = 1.38.10^{-23}$ J/K is the Boltzmann constant, and T is temperature.

III. Result and Discussion

Temperature dependent bandgap shows significant band gap reduction with increase in the compositions of indium and temperature by Vashni. The results when compared to previous experimental works matches for each of the compositions of Indium in InGaAs. This temperature dependent band gaps were calculated using the method described earlier.

Tables 5 give the summary of the Band gap of InGaAs for varying compositions of Indium.

Table 4: Band gap values of different concentrations of Indium at different Temperature

Bandgap of InGaAs	temperature	0 K	100 K	200 K`	300 K	400 K	500 K	600 K
$In_{0.53}Ga_{0.47}As$ (eV)		0.8161	0.800	0.772	0.736	0.7001	0.6640	0.6267
$In_{0.60}Ga_{0.40}As$ (eV)		0.7433	0.7276	0.6993	0.6668	0.6323	0.5967	0.5605
$In_{0.70}Ga_{0.30}As$ (eV)		0.6474	0.6321	0.6050	0.5742	0.5418	0.5084	0.4745
$In_{0.80}Ga_{0.20}As$ (eV)		0.5611	0.5461	0.5202	0.4912	0.4608	0.4296	0.3980
$In_{0.90}Ga_{0.10}As$ (eV)		0.4843	0.4696	0.4450	0.4177	0.3893	0.3604	0.3310
$In_{0.95}Ga_{0.05}As$ (eV)		0.4494	0.4350	0.4110	0.3846	0.3572	0.3293	0.3011

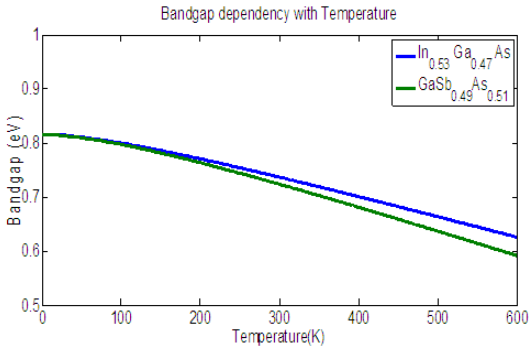

Figures 1: Band gap dependency as a function of temperature

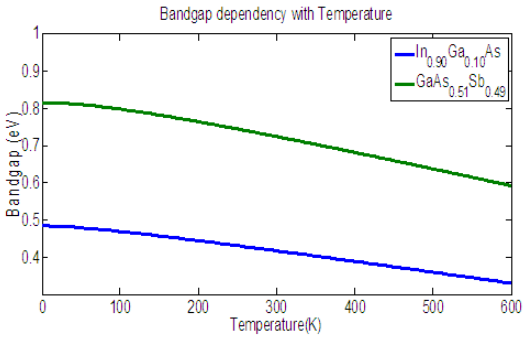

Figures 2: Band gap dependency as a function of temperature

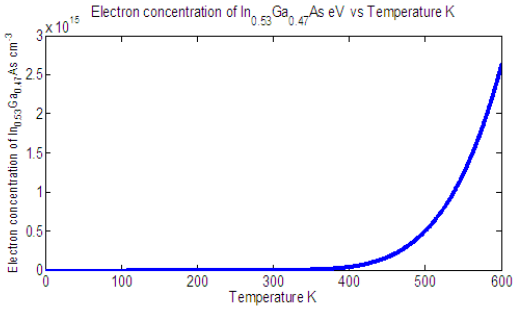

Figure 3 : Electron/Hole as a function of Temperature for $In_{0.53}Ga_{0.47}$ As

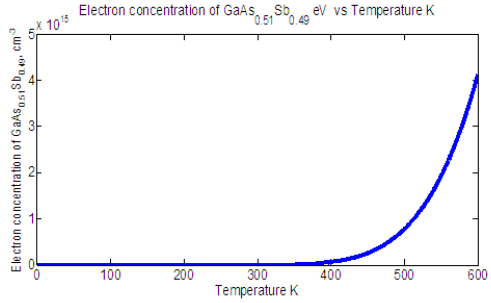

Figure 4: Electron/Hole as a function of Temperature for $GaAs_{0.51}Sb_{0.49}$

Figures 1 and 2 illustrate the temperature dependency of both InGaAs and GaAsSb at specific concentration of Indium. It reveals that as the temperature induced on these materials is increased, the band gap of these materials reduces. When the indium concentration was 0.53 at 0K, the band gap was about 0.815 eV. This value deceases to about 0.489 eV for 0.9 composition of Indium at 0 K. Figure 3 and 4 illustrate the electron/hole concentration for an intrinsic semiconductor of $In_{0.53}Ga_{0.47}As$ and $GaAs_{0.51}Sb_{0.49}$ at varying temperature. It reveals that there was an exponential rise in the electron- hole concentration as the temperature increases. This implies that at higher concentration, more electron-hole concentration at the conduction and valence band will be formed.

At low concentration, we observe that there concentration of electron/hole in the intrinsic semiconductor increased linearly with temperature. But increasing the range of temperature we observe the curves form. At 300 K we have the electron/hole concentration for $In_{0.53}Ga_{0.47}As$ and $GaAs_{0.51}Sb_{0.49}$ to be 7.2189e+011and 1.0492e+012 respectively. This implies that $In_{0.53}Ga_{0.47}As$ semiconductor has less electron/hole compared to that of $GaAs_{0.51}Sb_{0.49}$ semiconductor.

Tables 4.2 shows the effective masses, effective density of states for the conduction and valence band and the intrinsic carrier concentration for GaAs, GaSb, InAs, $In_{0.53}Ga_{0.47}As$ and $GaAs_{0.51}Sb_{0.49}$ at 300K. In the case of the valence band, only heavy and light hole bands were considered as the spin orbit band is sufficiently shifted, it can be ignored. Table 6 gives the summary of the intrinsic properties of InGaAs and GaAsSb quantum well

Table 6: Summary of the effective mass, effective density of state for conduction, valence band, and intrinsic carrier concentration for GaAs, InAs, GaSb, $In_{0.53}Ga_{0.47}As$ and $GaAs_{0.51}Sb_{0.49}$at 300K

Compounds/ Alloys	m_c	m_v	E_g	N_c	N_v	n_i
GaAs	$0.067m_0$	0.4722	1.4225	4.3530e+017	8.1449e+018	2.1390e+006
InAs	$0.026m_0$	0.4044	0.3538	1.0523e+017	6.4551e+018	8.8145e+014
GaSb	$0.041m_0$	0.2939	0.7267	2.0838e+017	3.9995e+018	7.2155e+011
$In_{0.53}Ga_{0.47}As$	0.0365	0.4337	0.7373	1.7501e+017	7.1684e+018	7.2189e+011
$GaAs_{0.51}Sb_{0.49}$	0.0511	0.3640	0.7242	2.9008e+017	5.5125e+018	1.0492e+012

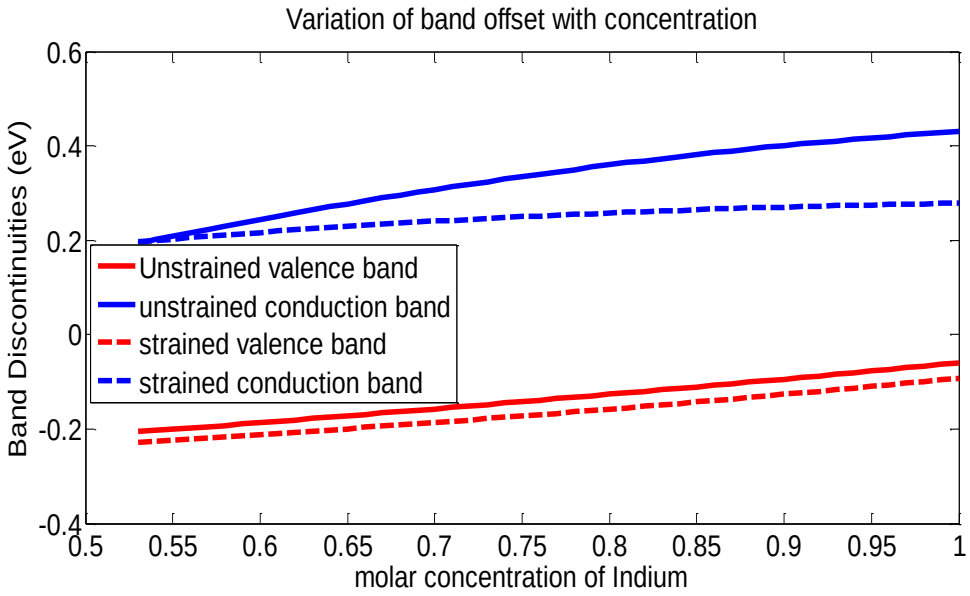

Figure 5: Calculated band offset of the conduction and valence for the compressively strained $Ga_{1-y}In_yAs$ / $GaAs_{0.51}Sb_{0.49}$ type II quantum well.

Figure 5 and 6 shows that as the concentration of Indium is increased, the band offset increases because of the decrease in the band gap of the composite alloy of InGaAs. When the material was strained, there was an improvement in the conduction band and a decrease in the valence band.

From the figures, the ratio of the discontinuous in the band reveals that the linearity in the band discontinuity changes at lower concentration of the indium in InGaAs. At 0.55 - 0.6 molar concentration of Indium, we obtain something like a curve. This will be seen clearly if we plot at lower molar concentration of Indium

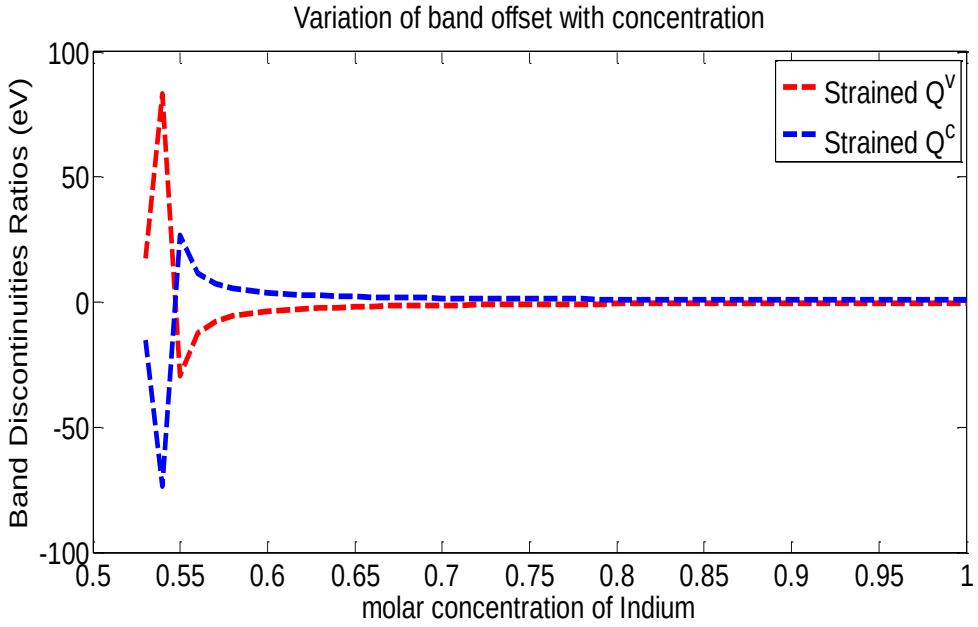

Figure 6: Calculated band offset ratios of Q^v *and* Q^c for the compressively strained $Ga_{1-y}In_yAs$ / $GaAs_{0.51}Sb_{0.49}$ type II quantum well. The curve shows that as the concentration of Indium is increased

Varying the composition of Indium in InGaAs, the conduction band offset can be computed for both strained and unstrained seminconuctor. The table below gives the conduction band offset for different molar concentration of Indium Arsenide in Gallium Indium Arsenide using the solid model theory

Table 7: Band offset values at different symmetric well masses

Composition of Indium (x)	Mass of the well	Unstrained conduction Band Offset (eV)	Strained conduction band offset (eV)
0.53	0.0475	0.1929	0.1960
0.55	0.0467	0.2080	0.2020
0.60	0.0446	0.2439	0.2158
0.65	0.0424	0.2770	0.2282
0.70	0.0402	0.3073	0.2395
0.75	0.0380	0.3348	0.2496
0.80	0.0357	0.3595	0.2588
0.85	0.0333	0.3814	0.2670
0.90	0.0309	0.4006	0.2744
0.95	0.0285	0.4169	0.2810
1.00	0.0260	0.4305	0.2870

IV. Conclusion

Model solid theory was employed to determine the band discontinuities as well as the ratio of the band offsets. This theory is similar to the k.p theorem in perturbation theory. It is easy and explicit in usage.

The transport in the semiconducting material were also analyzed to obtain the drift and the diffusion current, the mobility, carrier concentration, type of the semiconductors were also determine.

The effect of the increase concentration of the indium doping material at varying concentration were also analyzed critically for both strained and unstrained material.

References

[1]. Chris G. Van de Walle, Richard M. Martin. Theoretical calculations of heterojunction discontinuities in the Si/Ge system. PHYSICAL REVIEW B (1986) VOLUME 34, NUMBER 8

[2]. https://www.quora.com/What-is-a-quantum-well

[3]. Yehuda B. Band, Yshai Avishai. Quantum Mechanics with Applications to Nanotechnology and Information Sciences, 2013. Oxford Academic Press.

[4]. P. N. Uppal, H. Kroemer. Molecular beam epitaxial growth of GaAs on Si (211). J. Appl. Phys., (1985) 58:2195-2203,

[5]. J. McKenna, F. K. Reinhart. Double-heterostructure GaAs /AlxGa1-xAs [110] p-n-junction-diode modulator. J. Appl. Phys., (1976) 47:2069-2078,

[6]. Vurgaffman I., Meyer J.R., Ram-Mohan L.R. Band parameters for III-V semiconductors and their alloys' Journal of Applied Physics, American Institute of Physics (2001). Vol.89 No. 11.

[7]. Su-Huai Wei and Alex Zunger. Calculated natural band offsets of all II–VI and III–V semiconductors: Chemical trends and the role of cation d orbitals. APPLIED PHYSICS LETTERS(1998) VOLUME 72, NUMBER 16

[8]. UMESH K. MISHRA and JASPRIT SINGH. Semiconductor Device Physics and Design' book Published by Springer, P.O. Box 17, 3300 AA Dordrecht,(2008) The Netherlands ISBN 978-1-4020-6480-7 (HB); ISBN 978-1-4020-6481-4 (e-book)
[9]. C.G Van de Walle. SiGe Heterojunction and band offset . PHYSICAL REVIEW B (1999)
[10]. Chris G. and Van de Walle Band lineup and deformation potentials in the model-solid theory. PHYSICAL REVIEW B (1989) VOLUME 39, NUMBER 3
[11]. SHUN LIEN CHUANG. physics of Optoelectronic Devices. Test book published by John Wiley & Sons. Inc,.(1995) United State of America 94-2470 I
[12]. Z. Chen,a) S. N. Mohammad, D.-G. Park, D. M. Diatezua, H. Morkoc, and Y. C. Chang. Band structure and confined energy levels of the Si3N4/Si/GaAs system. J. Appl. Phys. 82 (1), 1 July 1997, American Institute of Physics
[13]. Wang T.S., Tsai J.T., Lin K.I., Hwang J.S., Lin H.H., Chou L.C. Characterization of band gap in GaAsSb/GaAs heterojunction and band alignment in GaAsSb/GaAs multiple quantum wells. Materials Science and Engineering B Elsevier 147 (2008) 131–135
[14]. Ferdinand Scholz, Compound Semiconductors Physics, Technology, and Device Concepts. Book *Published by* Pan Stanford Publishing Pte. Ltd. Penthouse Level, Suntec Tower 3 8 Temasek Boulevard Singapore 038988
[15]. Craig Pryor. Eight –band calculation of Strained InAs/GaAs quantum dots compared with one-, four-, and six-band approximations PHYSICAL REVIEW B, 15 MARCH 1998-II, Vol. 57, Number 12

P Ugochukwu Joseph, C.I Oriaku, et. al. "Band Alignment of Type II Strained Ga〖As〗_x 〖Sb〗_(1-x)/〖Ga〗_y 〖In〗_(1-y) As Quantum Well on InP(001) substrate." *IOSR Journal of Applied Physics (IOSR-JAP)*, 13(4), 2021, pp. 08-14.